CORE ANALYSIS WITH TWO DIMENSIONAL NMR

Boqin Sun and Keh-Jim Dunn
ChevronTexaco Exploration and Production Technology Company

ABSTRACT

We developed several novel two-dimensional (2D) NMR core analysis techniques, which not only enhance the analysis of fluid-saturated rock samples, but also open up an unexplored area for petrophysical research. This is different from the conventional one-dimensional (1D) NMR core analysis, in which only the proton population versus relaxation times, i.e., $T_{1,2}$ distribution, is displayed to characterize the rock properties. In the new techniques, the proton population can be expressed in a 2D correlation map, where one axis is the relaxation time, and the other axis can be internal field gradient, diffusion coefficient, or proton chemical shift. When the diffusion coefficient is used as the axis, the oil and water in the pore space can be separated in a 2D display. Using a Magic Angle Spinning technique, which removes the internal magnetic fields caused by the susceptibility contrast between solid matrix and pore fluids, the proton population can be displayed as a function of high-resolution proton NMR spectrum and T_1 or T_2 relaxation time in a 2D plot. This T1-MAS 2D NMR technique provides a possible way to study the surface wettability. Several experimental examples are presented to illustrate the two dimensional NMR techniques.

INTRODUCTION

Nuclear magnetic resonance (NMR) technology has been successfully applied to petro-physical studies of porous media. Among these applications, NMR relaxometry using the CPMG pulse sequence at low fields (600 kHz~2MHz) has been routinely used to estimate porosity, irreducible water saturation, permeability, and pore size distribution of rocks [1]. Combined with NMR diffusion measurements, NMR relaxometry has also been extended to perform fluid typing and oil viscosity estimation [2].

The successful applications of fluid typing techniques depend not only on the properties of the fluids in porous media, but also on the properties of its solid matrix [3]. This is because the relaxation time of hydrogen nuclei of the fluid is related to three factors: bulk $T_{1,2}$ relaxation, surface relaxation, and molecular diffusion. The bulk relaxation (T_{2B}) characterizes the process of energy transfer of spin nuclei through the coupling with lattice. The relaxation time is related to the dipolar coupling between spins, Larmor frequency, and degree of the random motion. The surface relaxation (T_{2S}) represents the interaction of molecules in the pore fluid with the solid matrix, and is greatly enhanced by the presence of paramagnetic impurities at the pore-solid interface. The surface relaxation time is related to the surface relaxivity and the surface-to-volume ratio of the pore space. The effect of molecular diffusion (T_{2D}) to the spin is related to the diffusion coefficient of the molecule, the magnetic field gradient, and the inter-echo spacing of a CPMG sequence. The experimentally measured apparent relaxation time (T_{2a}) is given by

$$\frac{1}{T_{2a}} = \frac{1}{T_{2B}} + \frac{1}{T_{2D}} + \frac{1}{T_{2S}} \approx \frac{1}{T_{2B}} + \frac{D(gG_aT_E)^2}{12} + r\frac{S}{V}, \quad (1)$$

where r is the surface relaxivity, T_E is the echo spacing of a CPMG sequence, G_a is the apparent averaged field gradient, and g is the gyromagnetic ratio.

The diffusion term given in equation (1) is a rough approximation. It is strictly valid only for an infinite fluid medium, and approximately valid for the diffusion of molecules in fluid-saturated porous media. The result of a restricted diffusion yields a time dependent diffusion constant, which in general is very difficult to solve precisely. Only in periodic porous media, Bergman and Dunn have theoretically solved the diffusion equation using Fourier expansion [4]. Normally, such diffusion effect is measured experimentally. If the diffusion time is short, then the approximation made in using the diffusion term in equation (1) is valid.

With the additional complexity of fluid properties, it is often a great challenge for the current one-dimensional relaxometry NMR to perform proper fluid typing in core samples. It is quite natural, then, to think of extending the current application into two-dimensional NMR. Such a 2D methodology has been widely used in conventional high-field NMR for solving macro-molecular structures. For example, in conventional high-resolution NMR, hydrogen chemical shift has been widely used to distinguish specimen of a mixture. As we know, the chemical shift difference between water peak and the aliphatic oil peak is about 4 ppm in a typical ^{1}H high-resolution NMR spectrum. A possible approach to our problem is to combine high field NMR spectroscopy with the low field NMR relaxometry.

However, proton NMR spectra of rock samples typically show a featureless broad line. From these spectra, we cannot distinguish oil from water using chemical shift differences. The line broadening in a ^{1}H spectrum is usually caused by magnetic susceptibility contrast between solid grains and pore fluid. This magnetic susceptibility contrast and the pore geometry often generate large internal field gradients across the pore volume [3,5]. In order to obtain high-resolution ^{1}H NMR spectra of rock samples, we have to remove these internal field gradients, or susceptibility line broadening.

We present here two novel two-dimensional NMR core analysis techniques. One is the Relaxation-Diffusion 2D (or RD2D) NMR method for probing internal field gradients, and the other is the T1-MAS (magic angle spinning) 2D NMR method for fluid typing. In the case for internal field gradient and T_2, the proton population can be displayed as a 2D NMR map as a function of the internal field gradient and T_2 (reflecting pore size), where the proton population is plotted along the third axis. When the axis for internal field gradient is replaced with the diffusion coefficient for the pore fluids, the oil and water in the pore space can be separated in a 2D display. When the magic angle spinning (MAS) technique is applied to remove the internal magnetic field, the proton population can be displayed as a function of high-resolution proton NMR spectrum and T_1 or T_2 relaxation time in a 2D plot. T1-MAS 2D

NMR provides a way to study the surface wettability and to distinguish oil from water. Several experimental examples are presented to illustrate the 2D NMR techniques.

THEORY

In porous media, fluid is surrounded by grains with various susceptibilities and shapes. Under an external magnetic field, grains are magnetized and internal magnetic field gradients are induced inside the pores [5]. The internal field gradients cause two types of effects. First, they cause a large spread of the resonance frequency of proton nuclei in the fluid such that pore fluids with different proton chemical shifts cannot be distinguished. Second, the T_2 relaxation rate is enhanced because of the diffusion of spins in these field gradients.

T1-MAS 2D NMR

We can eliminate the first effect of line broadening by applying the magic angle spinning (MAS) technique to a fluid-saturated porous sample. Under MAS, the rock sample rotates around an axis inclined at an angle of arc cos $(3^{-1/2}) \approx 54.74^o$ with respect to the applied external magnetic field (see Figure 1A), which leads to an averaged zero internal field. The resulting NMR spectra can clearly separate the aliphatic oil peak from the water peak [5-9] (see Figure 2).

We then perform a T_1/T_2 measurement in the MAS framework to obtain T_1/T_2 distribution (or pore size distribution). For convenience, we have used the standard inversion-recovery pulse sequence to measure T_1 relaxation time shown in Figure 1B. After the proton magnetization is inverted by the application of a 180^o pulse, it starts to recover according to $1-2\exp(-t_w/T_1)$, where T_1 is the longitudinal relaxation time constant and t_w is the recovery time before the 90^o pulse. The 90^o pulse is used to produce the free-induction decay (FID) for signal reception. Because of magic angle spinning, the internal field undergoes periodic changes. When the internal field is positive, the magnetization starts to dephase, and it refocuses when the internal field becomes negative (similar to CPMG). At the end of each rotation cycle, spin echo appears in the FID, and is traditionally called rotational echo. In the MAS framework, the FID signal is a train of rotational echoes, and the Fourier transformation of the FID signal yields a high-resolution, water-oil-separated spectrum. The intensity of each peak is modulated by a factor of $1-2\exp(-t_w/T_1)$. Using a set of recovery time t_w's, we are able to obtain T_1 recovery curve for each peak in the high-resolution MAS spectrum, which can be expressed as

$$s(w, tw_k) = \sum_n \sum_{j=1}^{N_R} a_{n,j} f_n(w - w_n) e^{-tw_k/T_{1,j}} \text{ , (k = 1,…,M)} \qquad (2)$$

where w denotes frequency variable in a chemical shift spectrum, w_n is the frequency of n-th peak, $f(w\text{-}w_n)$ is the shape of the n-th peak, M is number of wait-times, and $a_{n,j}$ gives the T_1 distribution for the n-th peak in a set of N_R pre-selected T_1 values. If we perform a T_1 inversion for every frequency (chemical shift) in the spectrum, the sequential arrangement of

all T_1 distributions along the chemical shift dimension yields a T1-MAS 2D spectrum of the rock sample.

Relaxation-Diffusion 2D (RD2D) NMR

To quantify the second effect of the enhanced T_2 relaxation rate due to spin diffusion in the internal field gradients, we develop a Relaxation-Diffusion 2D (RD2D) NMR approach. This approach allows us to decouple diffusion effects from the apparent T_2 relaxation and display the end results in a 2D manner. This methodology and the format of data representations permit us to identify and characterize the properties of the pore fluids and the pore network quite easily. In the following, we shall show such methodology applied to the analysis of the internal field gradient distribution as a function of different relaxation times. It can be easily extended to the analysis of the distribution of diffusion coefficient of pore fluids as a function of different relaxation times (or pore sizes). The latter can be used for easy fluid typing based on the contrast of their diffusion coefficients.

To extract information of internal field gradient from regular CPMG is very difficult [10-13]. However, we develop a new technique, which makes extracting such information possible. We devise a modified CPMG sequence where we split a regular CPMG into two parts and run a 2D experiment. We use minimum echo spacing (TE_2) in the second part of the sequence such that the diffusion effect is minimized. The decay curve of the magnetization during this period mainly gives the apparent T_2 distribution. However the echo spacing (TE_1) of the first part of width t_0 changes from a minimum TE to a maximum TE allowed (see Figure 3). This can be accomplished by changing the number of 180^o pulses. The change of the echo spacing corresponds to the second dimension that gives either diffusion coefficients of the pore fluids or the field gradient distribution of the rock. In other words, we can correlate the diffusion parameter to T_2 relaxation time. For example, a typical minimum echo spacing of a low field spectrometer is about 200μs. If we use a maximum echo spacing of 10ms, we can set t_0 to be 10ms and change the number of 180^o pulses from 50 to 1 to obtain 50 different sets of CPMG echo trains. The first echo amplitude of each echo train received during the second part of the sequence is attenuated only by the diffusion process occurred during the first part of the sequence.

Once we obtained a 2D set of echo trains, we apply inversion algorithm to obtain a 2D diffusion and T_2 correlation spectrum of a rock. For l-th TE_1 value, the i-th echo intensity (b_{li}) received during the second part of the sequence can be written as

$$b_{li} = \sum_{j=1}^{N_R} f_{lj} e^{-(t_i + t_0)/T_j} + e_i, \quad i = 1, \cdots, \mathrm{N_E} \text{ and } l = 1, \cdots, \mathrm{N_{TE}}, \tag{3}$$

where T_j is a set of N_R pre-selected T_2 relaxation times equally spaced on a logarithmic scale, f_{lj} is the set of amplitude corresponding to T_j for the l-th TE_1 value, N_E is number of echoes in an echo train, N_{TE} is number of TE_1's used in the second dimension, and e_i is the error between the inversion model and data. As we have mentioned that the f_{lj} is further modulated by the decay caused by molecular diffusion occurred during the first part of the

sequence in a rock sample. Figure 4 shows an example of variation of f_{lj} as function of TE_1. This variation can be further decomposed to

$$f_{lj} = \sum_{k=1}^{N_g} p_{jk}(g_k) e^{-Dt_0(gg_k TE_l)^2/12} + e_l, \quad j = 1, \cdots, \mathrm{N_R} \text{ and } l = 1, \cdots, \mathrm{N_{TE}}, \tag{4}$$

where N_g is the number of pre-selected gradient components, g_k, equally spaced on a logarithmic scale, e_i is the error between the model and the measured data, and N_R is the number of pre-selected T_2 relaxation times. The p_{jk} matrix gives the 2D-correlation distribution between the T_2 (or pore size) and the apparent internal field gradient. Note that we have assumed that the diffusion coefficient of the fluid is known and the diffusion process in a pore is unrestricted. However even these conditions are not completely true, they only affect the size of the G axis scale.

EXPERIMENTAL

MAS experiments were performed with a Bruker Instruments 4 mm MAS probe. The zirconia rotor size is 4 mm in O.D. and 20 mm in length. It can hold about 170 mg of crushed rock sample. The spinning speed was about 10 kHz. The 90^o pulse length varies between 3 and 6 μs depending on individual core plug.

Standard inversion-recovery pulse sequence is shown in Figure 1B. The recovery time set used in our experiments is [0.2, 0.4, 0.6, 0.8, 1, 2, 3, 5, 10, 20, 50, 100, 200, 500, 1000, 2000] ms. The T_1 inversion used is based on the Butler, Reeds, and Dawson (BRD) method.

For the internal field gradient measurement, we acquired all 2D data on MARAN 2MHz spectrometer. The 90^o pulse length was 8.3 μs and 180^o pulse length was 16.5 μs. The field inhomogeneity is less than 10Hz. The temperature of the sample holder is maintained at 26^oC. Wait time of 5 seconds was used for all measurements. The minimum echo spacing was 174μs and the maximum echo spacing was 10.2ms. Depending on the T_2 distribution, number of echoes varied between 2,000 and 10,000. The RD2D pulse sequence used to measure 2D-correlation distribution between internal gradient field and T_2 distribution is shown in Figure 3. A regular CPMG sequence is split into two parts. The first part lasts for t_0 time. During this period the echo spacing, TE_1, increases as the number of 180^o pulses reduces. After the first period, CPMG echo trains are acquired with minimum echo spacing, TE_2.

RESULTS

T1-MAS 2D Spectrum of Diatomite

Figure 5 shows the comparison of T1-MAS 2D spectra of fresh, flooded, and extracted core plugs. Because MAS removes the line broadening caused by internal fields, we are able to distinguish oil from water using a MAS spectrum. The first dimension in the figures is the chemical shift that is used to identify the oil peak (1.4 ppm) and the water peak (5.1 ppm). The second dimension is the T_1 relaxation time. The third dimension is the corresponding

amplitude. The left panel shows the 3D surfaces of T1-MAS 2D spectra and the right panel is their contours with projections attached. The projection is simply given by the sum of all amplitudes along either the chemical shift or the relaxation time dimension. The intensity of each figure is arbitrarily scaled for best viewing effect in terms of shape. Only the relative intensity within the same figure is meaningful.

The T1-MAS 2D spectrum of the fresh core shows that the chemical shift of the (main) aliphatic oil peak is about 1.4 ppm and its T_1 peak is located at about 76 ms (see the first row of Figure 5). The aromatic oil peak is about 7 ppm (not obvious) and the T_1 of the peak is about 76 ms too. There might be a small amount of oil whose T_1 is around 1 ms. The water peak is at 5.1 ppm and it has two T_1 peaks. The short T_1 water peak is around 1 ms while the long T_1 water peak is at about 550 ms. Since the amplitude of the long T_1 water peak is small, it is buried in the up shoulder of a 1D T_1 distribution and is not easily discernible (Note that the 1D T_1 distribution is shown at the right edge of the figure, which is the T_1 projection along the chemical shift dimension).

After the Dean-Stark extraction experiment of the core plug, the oil peak disappeared from the T1-MAS 2D spectrum (see the middle row of Figure 5). However the long T_1 water peak remains unchanged and the short T_1 peak increases to 13ms. Note that the core plug after extraction was dried and there should not be any free water in the core plug. This peak may arise from either the absorbed moisture from air or residual water imbedded in non-permeable large size pores in the diatomite. The fluid trapped in these pores is water. The widely distributed short T_1 peak at 5 ppm indicates that it is water either capillary bound in small pores or chemically bound to solid surfaces.

The third row of Figure 5 shows the T1-MAS 2D spectrum of brine flooded core plug. T_1 relaxation time of the oil peak increases to about 174 ms and the susceptibility broadening reduces by a factor of 2. The intensity of aromatic oil peak seems reduced. The intensity of the short T_1 water peak increases a lot while its T_1 relaxation time also increases from 1ms to about 2.4ms. However, the long T_1 water peak remains unchanged. This clearly indicates that the surface of the solid matrix is mainly water wet. After water gets into pores, the water molecules form hydrogen bonds with the surface of the solid matrix of diatomite formation and form a layer of water. That will push oil to the middle of a pore where the magnetic field is more homogeneous and the susceptibility broadening is reduced. This explains that the line width of the oil peak in the chemical shift dimension becomes narrow after flooding. As the water layer becomes thick, the surface relaxivity of oil droplet decreases, leading to increasing of T_1 relaxation time of the oil.

The change of T_1 distribution before and after the flooding experiment is very similar to the change of T_2 distribution measured at low field. After the flooding the water saturation increases and only small amount of oil was replaced by water.

Internal Field Gradient

Figure 6 (A) shows an example of RD2D NMR with water-saturated sandstone where moderate paramagnetic impurities are present. The RD2D plot displays the signal intensity as a function of T_2 relaxation times and internal field gradients. Note that the signal intensity is related to hydrogen population and the T_2 relaxation time reflects pore size. The volume integration of the 2D plot gives the porosity of the sample. The cross section view at a fixed T_{2j} gives the distribution of internal gradients for that pore size. Since the long T_2 fluid resides in large pores while the short T_2 fluid resides in small pores, one might think that fluids with a large field gradient should reside in small pores while fluids with small field gradient should be in large pores. This statement is true only if the self-diffusion is in an unrestricted environment. Such a condition is more difficult to satisfy in small pores. When this condition is violated, the apparent field gradient will be smaller than the actual value. The 2D pattern of RD2D is also related to how the grains are packed or how pores are connected. The spread of the distribution can be as large as a few hundred Gausses across a pore with large bulk grain magnetic susceptibility. The conventional T_2 distribution and mercury porosimetry curve of the sample show that there is no obvious bimodal structure. The RD2D distribution is also very smooth and featureless. However Figure 6 (B) shows another example of a RD2D distribution with a different sandstone core sample from a different oil field, which clearly indicates two well-separated peaks in the 2D plot.

The RD2D pulse sequence can also be applied to obtain a 2D spectrum with the T_2 relaxation time as the first dimension and the diffusion coefficient as the second dimension if we know the internal field gradient or apply an external magnetic field gradient to core plug samples. Usually the diffusion coefficient of oil is very different from that of water, especially in heavy oil reservoir. At a given temperature, the diffusion coefficient of water should be a constant. However, for crude oil, it can be a distribution. We can use the water peak to estimate the internal field gradient and then use the information to further obtain the diffusion coefficient distribution for oil. Caution should be taken while we use this method to study the oil diffusion coefficient. First, the measurement of RD2D data should satisfy non-restricted diffusion condition. Second, for water-wet formation, the measured apparent internal field gradient of water should be larger than that of the oil since oil usually sits in the middle of pores as droplet. Figure 7 shows an example of RD2D spectrum of internal field gradient distribution for a fresh diatomite core plug containing crude oil, where the inversion was carried out by assuming a single diffusion coefficient with a value for water at room temperature. The right peak in the gradient dmension is from irreducible water saturation while the left side peak is from crude oil. This explains the separation of the apparent field gradient of oil from water. It roughly follows the following relationship:

$$G_{a,oil} = G_{a,water}\sqrt{\frac{D_{oil}}{D_{water}}}, \tag{5}$$

where D_{oil} and D_{water} are the diffusion coefficients of oil and water, respectively. $G_{a,water}$ is the apparent internal field gradient if the imbedded fluid is water, and $G_{a,oil}$ is the apparent internal field gradient of oil. This example shows that RD2D method can be used to

distinguish heavy oil from irreducible water in a core plug when they both overlap in a 1D NMR display.

The mean (or effective) apparent gradient field inside a pore can be approximately expressed as

$$G_0 \propto \Delta B_0 \Big/ \langle d \rangle, \tag{6}$$

where <d> is the mean diameter of a pore [14]. We have also measured the susceptibility of the two samples and their mean pore size. Using the data we have computed, the mean gradients of the two samples and the results are similar to the mean value of RD2D.

The techniques for obtaining the distribution of diffusion coefficients need not be limited to the use of pulsed field gradients with varying τ. Other techniques, such as stimulated echo technique proposed by Tanner [14] with varying diffusion time, pulsed field gradient, or pulse width have shown to be successful in obtaining a distribution of diffusion coefficients.

CONCLUSIONS

- Our T1-MAS 2D (T1 Magic Angle Spinning – two-dimensional) NMR study showed the ability to distinguish water and oil and the possibility of wettability change during the flooding experiment.

- RD2D (Relaxation-Diffusion two-dimensional) NMR allows us to measure apparent internal gradient field. We have seen very interesting 2D patterns of these cores. The measured field gradient is compatible with the numerical calculation. The same method can also be used to measure the diffusion coefficients as a function of pore size. The latter can be used for identification of various pore fluids based on the contrast of their diffusion coefficients.

REFERENCES

1. Dunn, K-J., Bergman, D.J., and LaTorraca, G.A., Nuclear Magnetic Resonance--Petrophysical and Logging Applications, *Handbook of Geophysical Exploration*, Vol. 32, Pergamon, New York (2002).
2. Freedman, R., Sezginer, A., Flaum, M., Matteson, A., Lo, S., and Hirasaki, G.J., ., "A New NMR Method of Fluid Characterization in Reservoir Rocks: Experimental Confirmation and Simulation Results", SPE Paper63214, Society of Petroleum Engineers, Dallas, TX (2000).
3. Hurlimann, M.D., Effective Gradients in Porous Media due to Susceptibility Differences, *Journal of. Magnectic Resonance* **131**, 232 (1998).
4. Bergman, D.J., and Dunn, K-J., NMR of Diffusing Atoms in a Periodic Porous Media in the Presence of a Nonuniform Field Gradient, Phys. Rev. E **52**, 6516 1995.

5. Sun, B., and Dunn, K-J., Probing the internal field gradients in porous media, *Phy. Rev*. E **65**, 051309 (2002).
6. de Swiet, T. M., Tomaselli, M., Hurlimann, M. D., and Pines, A., In Situ NMR Analysis of Fluids Contained in Sedimentary Rock, *J. Magn. Reson.* **133**, 385-387 (1998).
7. Wilson, D. M., and LaTorraca, G. A., NMR magic angle sample spinning for measuring water and heavy oil saturation and high resolution relexaometry, *Symposium of Society of Core Analysts*, Paper 9923 (1999).
8. Hayashi, S., and Akiba, E., Nuclear Spin-Lattice Relaxation Mechanisms in Kaolinite Confirmed by Magic-Angle Spinning, *Solid State Nucl. Magn. Reson.,* **4**, 331-340 (1995).
9. Xiao, L., Du, Y., and Ye, C., "^{13}C Longitudinal Relaxation of Fluids Saturated in Oil Reservoir Cores by MAS NMR," *J. Colloid Interface Sci.* **164**, 495-497 (1994).
10. Appel, M., Freeman, J., Perkins, R.B., Hofman, J.P., Looyestijn, W.J., Slijkerman, W.F.J., and Volokitin, Y., Restricted Diffusion And Internal Magnetic Field Gradients, Society of Professional Well Log Analysts 40th Annual Logging Symposium, Paper FF, Oslo, Norway, May 30-June 3 (1999).
11. Shafer, J.L., Mardon, D., and Gardner, J., Diffusion Effects on NMR Response of Oil and Water in Rock: Impact of Internal Gradients, Symposium of Society of Core Analysts, Paper 9916, Golden, CO, August 1-4 (1999).
12. Zhang, G.Q., Hirasaki, G.J., and House, W.V., Internal Field Gradients in Porous Media, Society of Professional Well Log Analysts 41st Annual Symposium, paper AA, Dallas, TX., June 4-7 (2000).
13. Dunn, K-J., Appel, M., Freeman, J.J., Gardner, J.S., Hirasaki, G.J., Shafer, J.L., and Zhang, G., Interpretation of Restricted Diffusion and Internal Field Gradients in Rock Data, Society of Professional Well Log Analysts 42nd Annual Symposium, Paper AAA, Houston, TX., June 17-20 (2001).
14. J.E. Tanner, Use of the Stimulated Echo in NMR Diffusion Studies, J. Chem. Phys. **52**, 2523 (1970).

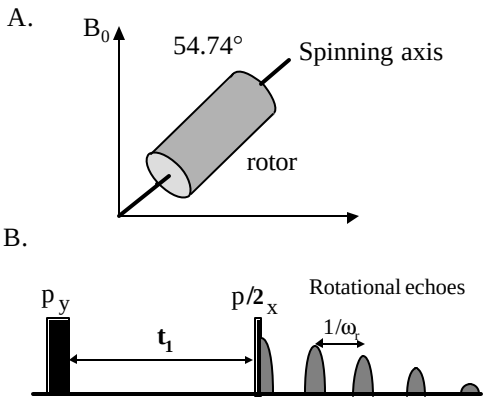

Figure 1. Diagram of T1-MAS 2D pulse sequence. (A) The magic angle spinning of rock samples. The rotor size is 4 mm in OD and 20mm in length. It holds about 170 mg of crushed rock sample and rotates at speed (ω_r) of 10 kHz. (B) The inversion recovery pulse sequence for T_1 measure-ment. The time t_1 varies from 0.2 ms to 2 seconds unevenly.

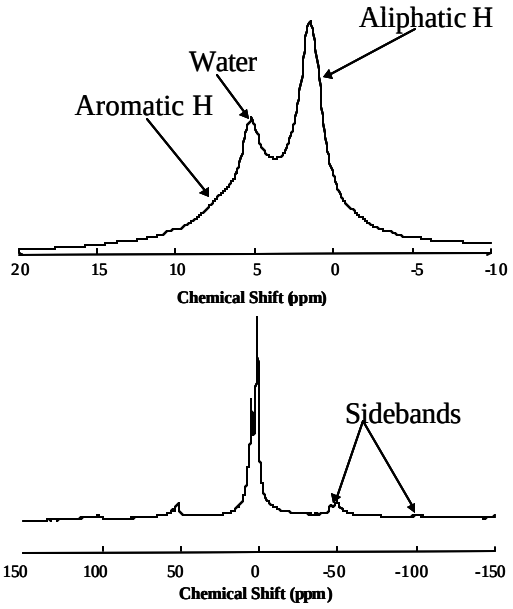

Figure 2. 1D MAS ^{1}H high-resolution spectrum of a rock sample, which clearly resolves water, oil aliphatic and aromatic protons. The top spectrum is the expansion of the bottom full spectrum.

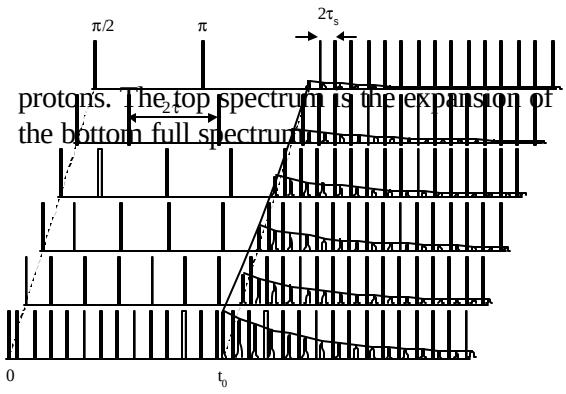

Figure 3. RD2D pulse sequence derived from CPMG sequence. The first part has a window width of t_0 where the echo spacing is varied from the smallest to the longest τ allowed, and the diffusion effect is encoded in the amplitudes corresponding to different relaxation times acquired during the second part of the sequence with smallest τ.

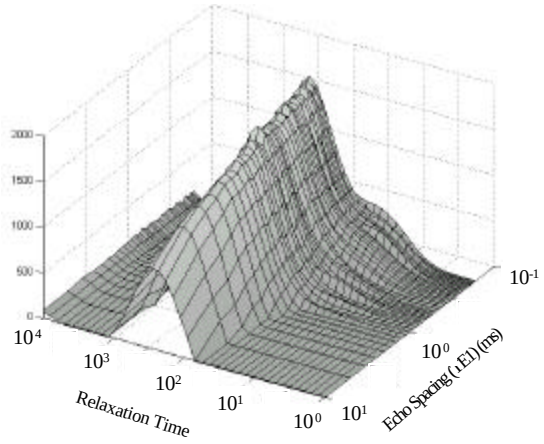

Figure 4. The T_2 distributions inverted from the CPMG data acquired in the second part of the RD2D sequence shown in Figure 3 vary with TE_1. It is clear that T_2 amplitudes monotonically decay with increasing of TE_1 due to diffusion effect encoded during the first period, t_0.

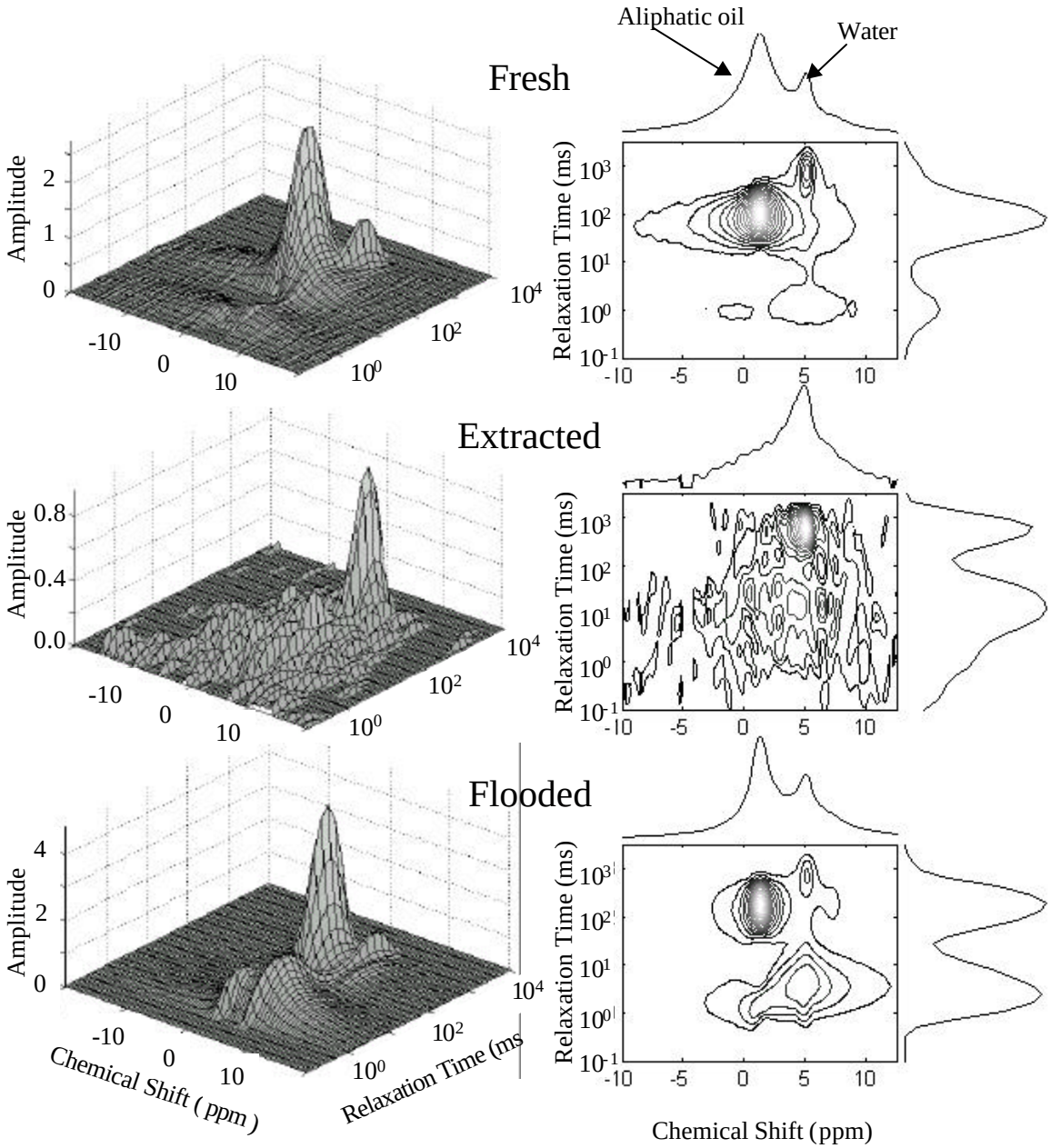

Figure 5. T1-MAS two-dimensional (2D) spectra of fresh, flooded, and extracted core plugs. The first dimension is the chemical shift that is used to identify the oil peak (1.4 ppm) and the water peak (5.1 ppm). The second dimension is the T_1 relaxation time that indicates the pore size. The left panel shows the 3D surfaces of T1-MAS 2D spectra and the right panel is their contours with projections attached. The intensity of each plot is arbitrarily scaled for best viewing effect in terms of shape. Only the relative intensity within the same plot is meaningful.

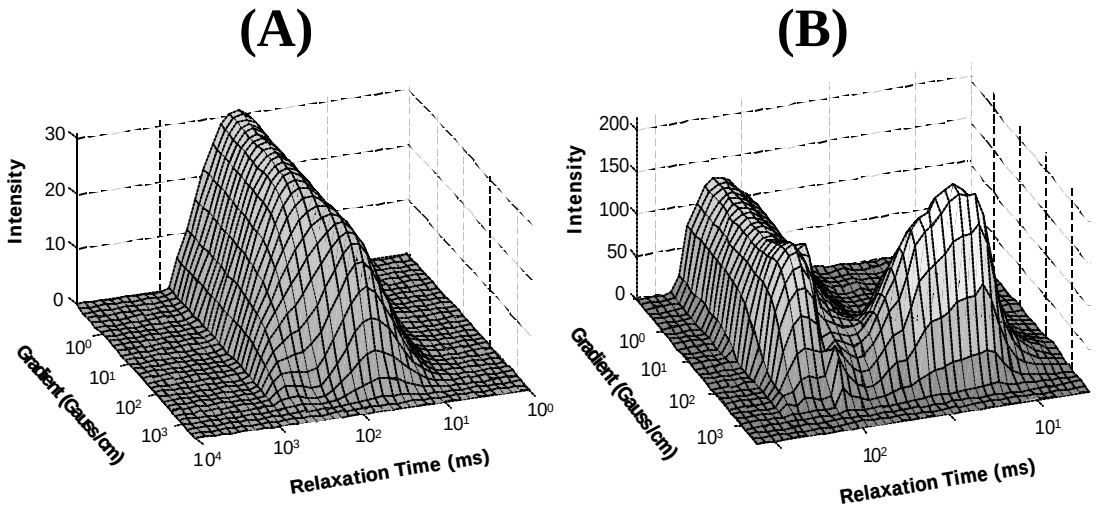

Figure 6. Examples of RD2D NMR spectra with water-saturated sandstone cores. Paramagnetic impurities are moderately present. The RD2D plot displays the signal intensity as a function of T_2 relaxation times and internal field gradients. The volume integration of the 2D plot gives the porosity of the sample. The cross section view at a fixed T_{2j} gives the distribution of internal gradients for that pore size. Two core plugs are from different oil fields.

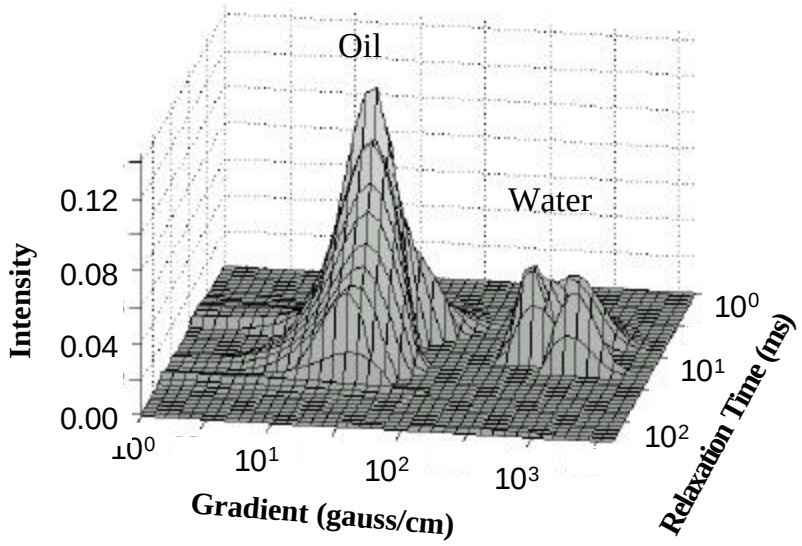

Figure 7. RD2D Spectrum of a fresh diatomite core plug containing crude oil. The right peak in the gradient dimension is from irreducible water saturation while the left peak is from the crude oil. In the 2D inversion, the diffusion coefficient of water at room temperature was used. This explains why the apparent field gradient of oil is smaller than that of the water peak.